FIFTH INTERNATIONAL CONGRESS ON SOUND AND VIBRATION

DECEMBER 15-18, 1997
ADELAIDE, SOUTH AUSTRALIA

ANALYSIS OF THE ACOUSTIC AND HYDRODYNAMIC FIELDS DOWNSTREAM OF A SHARP EDGED ORIFICE IN A FLOW DUCT SYSTEM FOR HIGHLY TURBULENT FLOWS

Rolf C. Pedersen and Michael P. Norton

Department of Mechanical and Materials Engineering
The University of Western Australia
Nedlands WA 6907 Australia

ABSTRACT

Methods developed in the frequency domain are used for quantifying the hydrodynamic and acoustic components of the internal wall pressure fluctuations downstream of a flow disturbance in a flow duct system. This paper examines in detail, for frequencies below the (1,0) higher order acoustic mode, the acoustic and hydrodynamic fields for air flow downstream of a sharp edged orifice in a cylindrical flow duct. Particular attention is paid to the effect of the presence of a downstream standing wave field and the transmission of energy through the orifice.

INTRODUCTION

Downstream of an orifice plate in a turbulent gas flow the flow field primarily consists of a separated flow region, a recovering flow region and a fully developed flow region. This paper furthers the work of Pedersen and Norton[1] and will consider in some detail the changes that the wall pressure spectrum undergoes as the flow field expands downstream of an orifice.

In depth studies of the wall pressure field downstream of an axisymmetric flow disturbance have been conducted by Kerschen and Johnston[2] and Agarwal[3] using an orifice and by Stahl[4] using an axisymmetric sudden expansion. These authors each examined the overall internal wall pressure field by taking measurements across a broad frequency range and examined in some detail the influence that the higher order acoustic modes have on the sound field. Agarwal[3] and Stahl[4] considered various axial locations across all regions whereas Kerschen and Johnston[2] only considered one location in the fully developed flow region. Stahl[4] and Kerschen and Johnston[2] recognised the influence felt by the presence of a standing wave field on the wall pressure field and so incorporated anechoic terminations in their experiments.

This investigation considers multiple axial locations and also incorporates an anechoic termination, however it is restricted to frequencies below the onset of the (1,0) higher order acoustic mode. This is a frequency region important from an acoustic fatigue perspective.

EXPERIMENTAL FACILITY AND REATTACHMENT DETERMINATION

A new experimental facility has been constructed at The University of Western Australia for this investigation. The facility consists of a 1.99 m (32 internal diameter) flanged steel test section with an internal diameter of 62.7 mm and a thickness of 5.2 mm. This section is downstream of a sharp edged orifice of 23 mm internal diameter. Air enters a large air receiver from a regulated compressed air supply at a constant mass flow rate governed by a choked globe valve. The air is then is forced through three 90° long radius bends then travels 11 internal diameters before it reaches the orifice. The test section contains 10 mm holes in sets of four with built up sides at numerous downstream locations. By reversing the test section, measurements may be obtained at 1, 2, 3, 4, 5, 6, 8, 12 and 18 internal diameters downstream of the orifice leading edge. Measurements may also be made upstream of the leading edge at -2 and -9 internal diameters. PCB 112A series pressure transducers were used and could be mounted flush with the internal pipe wall. Plugs made to the same dimensions as the transducers were fitted to the holes not being used for pressure measurements. Angular separations at each location of 45°, 90°, 135° and 180° are possible at each location.

The end conditions considered are an open flanged pipe (the test section end) and an anechoic termination. The termination is purpose built and commences at the pipe internal diameter before expanding past a conical pod. Acoustic absorption material up to 300 mm thick is used as an absorptive liner.

Initial measurements of basic flow parameters were made using a pitot tube aligned with the flow centre, a static tube and a thermocouple flush with the pipe wall. Figure 1 gives Mach numbers for the two flow cases calculated from compressible flow relations for an ideal gas with an expansion. It may be seen from Figure 1 that the flow conditions with each end condition are similar. From a peak Mach number of 0.9 the flow settles down to a Mach number of around 0.09 by 5 diameters downstream.

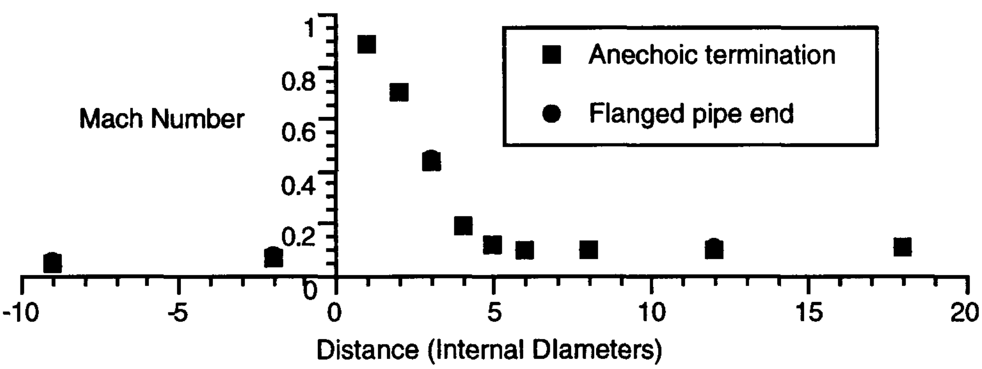

Figure 1 Mach numbers obtained from static and total pressure measurements at each axial location with a reference temperature at -2 diameters of 16°C for the 23 mm orifice

Critical to this investigation was the measurement of the reattachment location of the turbulent flow field. An acrylic section was devised to enable surface droplet flow visualisation to be carried out. This section also incorporated tufts at 20 mm intervals and static pressure tappings to provide confirmation of the surface droplet results. The effect of surface roughness was examined by lining the acrylic section with a thin layer of material of similar surface roughness to the test section and was found to have little effect.

For both end conditions the reattachment was thus determined to be at 195±5 mm downstream This corresponds to 9.6 to 10.1 step heights (pipe radius minus orifice radius) and 3.0 to 3.2 internal diameters. Clearly the 3 diameter measurement location was at reattachment.

Data has been acquired on a National Instruments NB-A2150F card mounted in a Macintosh computer and programmed using Labview. Signal processing has been performed using routines written in C and performed on a Unix machine. The National Instruments card features set sample rates with built in analogue and digital anti-aliasing filters. Data was acquired at either 8 or 12 kHz with a magnitude corrected Hanning window and 50% overlapped processing being used for each channel throughout the analysis.

The analysis makes use of shaded surface plots of autospectra and coherence functions. The linear interpolations between measurement locations are for visual effect and are intended to represent a qualitative trend rather than as a representation of component magnitude.

INTERNAL WALL PRESSURE FIELD DOWNSTREAM OF THE ORIFICE

The overall effect of the variation of the internal wall pressure fluctuations (IWPF) downstream of the orifice may be incorporated in a single figure. In Figure 2, the change from the flatter autospectra close to the orifice to a more peak - trough character and the rise in fall in magnitude as the flow reattaches and then proceeds downstream are clearly evident. The autospectra at 1 diameter is of distinctly reduced magnitude in comparison to those at 2 and 3 diameters. The reduced wall pressure fluctuation levels at 1 diameter suggest that the sound in this frequency band is not penetrating to this location. This would be expected owing to the fast flowing nature of the jet whose vena contracta is somewhat downstream of the orifice plane. Also the autospectra at 2 diameters is roughly double in magnitude to that at 3 diameters. This is surprising given that reattachment was determined to be at 3 diameters, at which it would be anticipated that the full force of the jet would be felt.

Downstream of reattachment, from 3 to 6 diameters, the key feature is the diminishing in magnitude of the autospectra towards a constant value as the distance increases from the source. Also the characteristic of the autospectra changes from that associated with broadband turbulence to a more peak - trough character. For 8 and 12 diameters downstream the overall magnitudes of the autospectra are fairly constant. The peaks and troughs in the autospectra are somewhat at variance. It is not clear whether this variance is due to a stationary or a propagating phenomena.

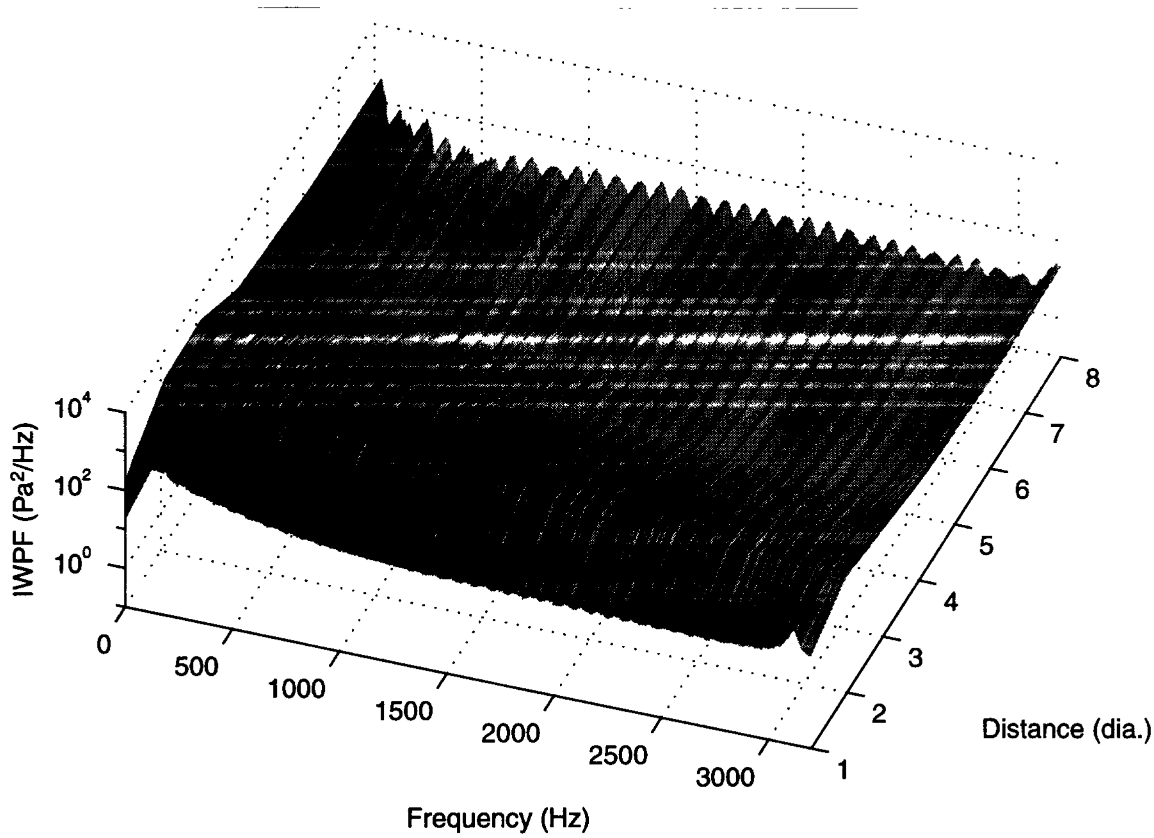

Figure 2 Autospectra of the internal wall pressure fluctuations (IWPF) measured at 1, 2, 3, 4, 5, 6 and 8 diameters with the anechoic termination end condition

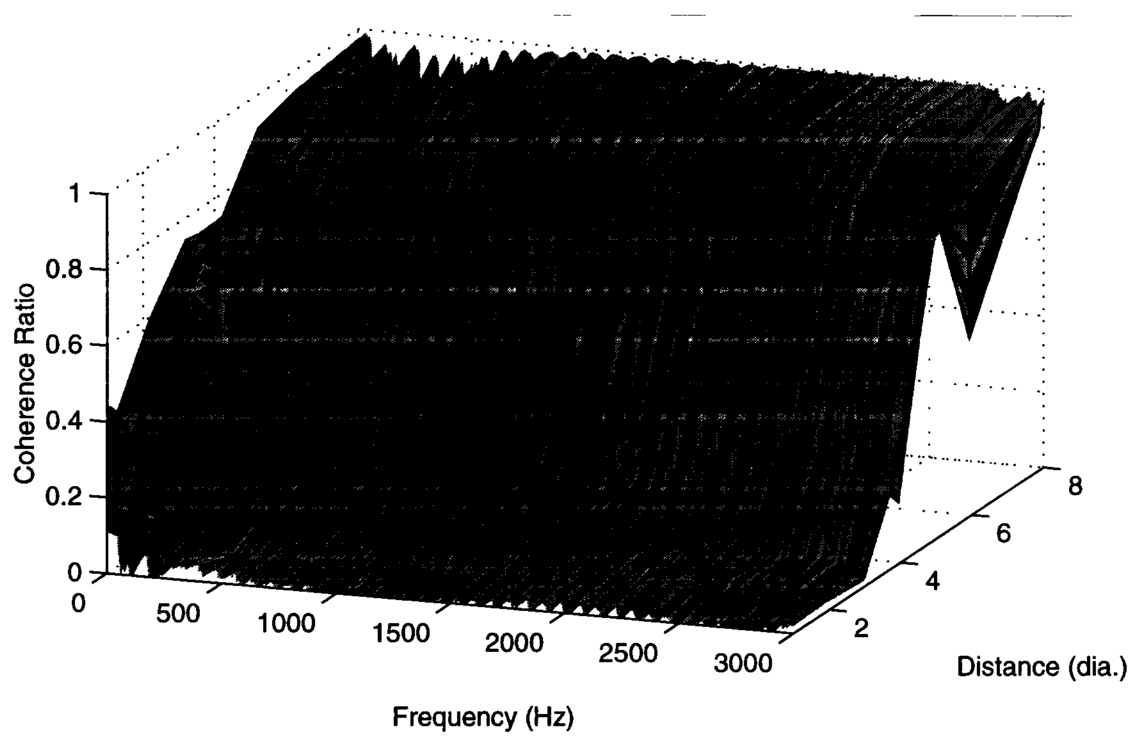

Figure 3 Coherence measured for 180° angular separations at 1, 2, 3, 4, 5, 6 and 8 diameters with the anechoic termination end condition

From Pedersen and Norton[1] the coherence between two locations at 180° angular separation on a pipe circumference are seen to minimise the correlated component on account of the finite spatial correlation of both turbulence and turbulence generated broadband noise. The results of the coherence at 180° of angular separation are presented in Figure 3. It may be seen that the magnitude of the coherence near the orifice commences at an extremely low value and stays to a constant low value to near reattachment at 3 diameters. This indicates that only a small portion of the autospectra measured in the flow separation region is correlated across the duct and indicates the large portion of uncorrelated phenomena present at these locations. From reattachment the coherence quickly rises and is very close to unity by 6 diameters downstream of the orifice. This indicates the dominance of the correlated signal portion at these locations.

From Pedersen and Norton[5], the time delay between two measurement locations a fixed distance apart may be determined from the gradient of the unwrapped phase.

$$\tau(\sec) = 360 \cdot \frac{\Delta\theta(°)}{\Delta f(Hz)} \qquad (1)$$

From equation 1 and the speed-distance-time relationship a mean propagation speed may be determined.

Using equation 1 it was evident that this dominating correlated signal portion at the downstream axial locations was due to a propagating correlated acoustic field. It is then evident from Figures 2 and 3 that this correlated acoustic field is not dominant close in to the orifice and that the uncorrelated hydrodynamic and uncorrelated acoustic components are.

EFFECT OF STANDING WAVES ON DOWNSTREAM WALL PRESSURE FIELD

The removal of the anechoic termination has a profound effect on the internal wall pressure field. Figure 4 clearly illustrates the presence of ridges in the autospectra occurring at discrete frequencies downstream of the orifice for 0 to 1000 Hz. These ridges are due to the standing waves that exist within the duct for the flanged pipe end condition. These standing waves dominate the wall pressure fluctuations downstream of reattachment and they appear to influence the flow in the separated flow region. It should be noted that these waves occur at almost the same frequency at each point along the duct. Also evident in Figure 4 is the mode shapes that these waves take on along the duct at each of their harmonic frequencies. With increasing downstream distance the modes cycle through peaks and troughs whose rough shape may be seen in the linear interpolations of the surface magnitude plot for each harmonic frequency. The figure is capped at 1000 Hz to avoid overly erroneous estimates of the mode shapes due to inadequate characterisation points.

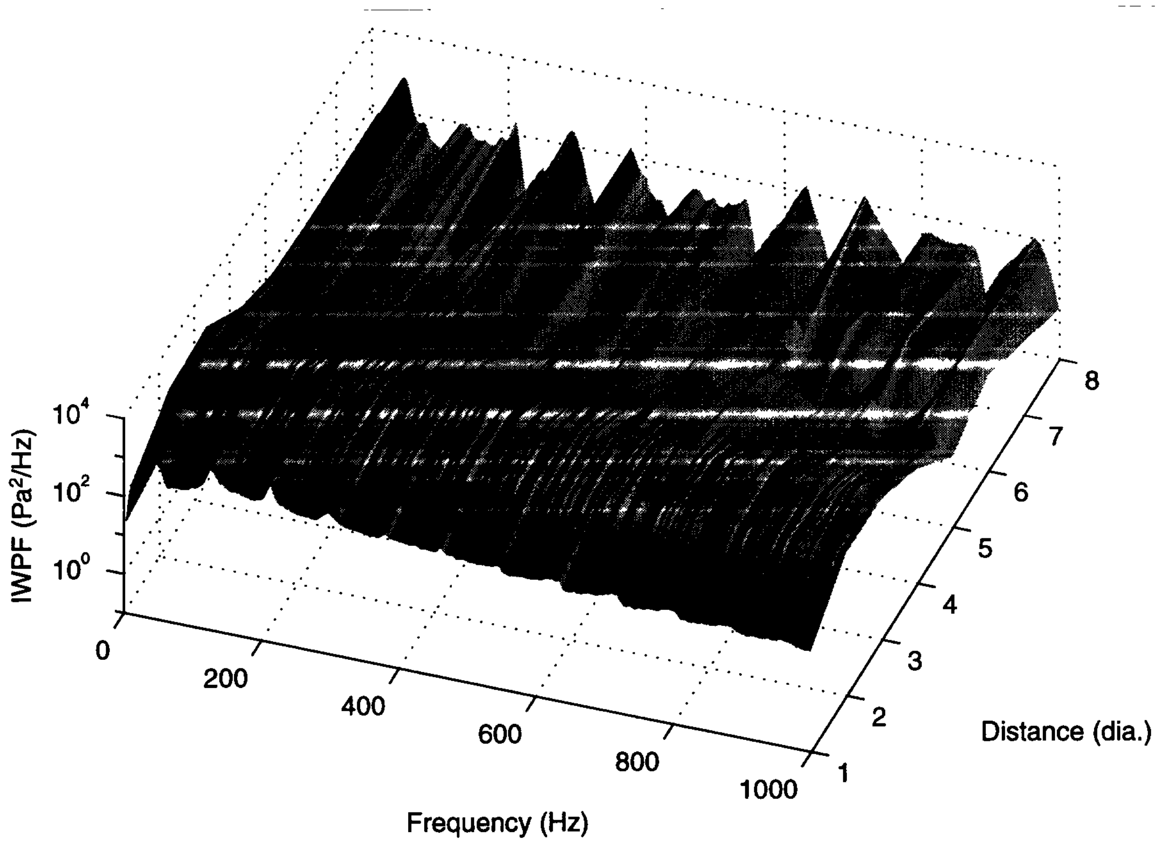

Figure 4 Autospectra of the internal wall pressure fluctuations (IWPF) measured at 1, 2, 3, 4, 5, 6 and 8 diameters with the flanged pipe end condition up to 1000 Hz

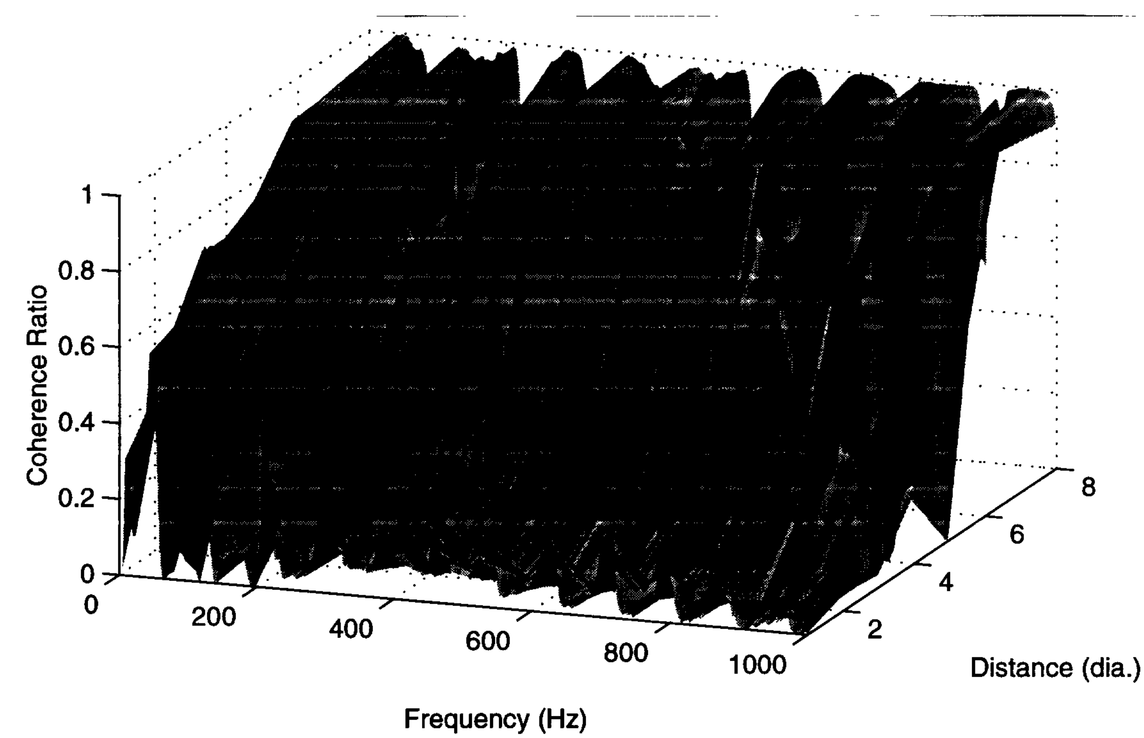

Figure 5 Coherence measured for 180° angular separations at 1, 2, 3, 4, 5, 6 and 8 diameters with the flanged pipe end condition

The effect that the standing waves have on the coherence between two transducers at 180° angular separation is evident in Figure 5. In comparison to Figure 3, the coherence is dominated by the coherent ridges associated with the mode shapes of the standing waves and this influence appears to extend to within the separated flow region.

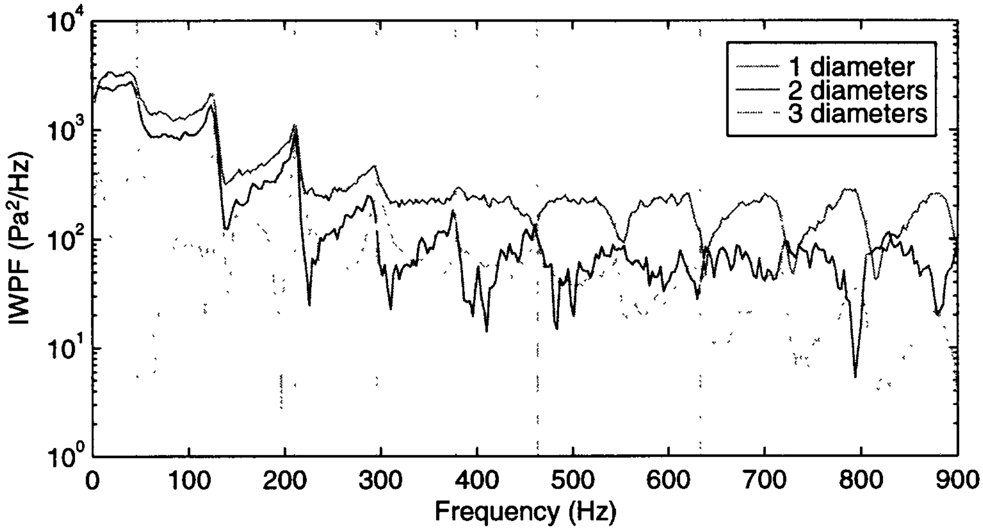

Figure 6 Cross spectra magnitudes of the internal wall pressure fluctuations (IWPF) at 1,2,3 diameters with the flanged pipe end condition

From Pedersen and Norton[1] the cross spectra magnitude between two coaxial measurement locations at a 180° angular separation for an axisymmetric system may be used to minimise the uncorrelated signal portion.

The cross spectra magnitudes between two transducers located at 180° angular separations at axial locations in the separated flow region are given in Figure 6 for the flanged pipe end condition. Also in Figure 6 are lines corresponding to the frequencies at which peak maxima occurred in the fully developed and recovering flow regions (as per Figures 4 and 5). From Figure 6 it is observed that the standing waves are in fact present within the flow separation region, confirming the supposition from Figure 5. This is evidenced by the peaks and troughs that are seen to align with the peak maxima from the downstream work. If a frequency shift associated with the change in flow conditions exists, it is not detectable over this frequency range. Examination of the cross spectra magnitudes for the case when the anechoic termination is fitted reveals that there is little evidence of any correlated phenomenon within the flow separation region.

THE INTERNAL WALL PRESSURE FIELD UPSTREAM OF THE ORIFICE

Figure 7 indicates narrow band spectral peaks present in the autospectra downstream of the orifice which are out of character with the rest of the wall pressure field It is suggested that these peaks are due to acoustic energy being transmitted through the orifice plate. In order to ascertain this, an examination has been made of the acoustic field upstream of the orifice.

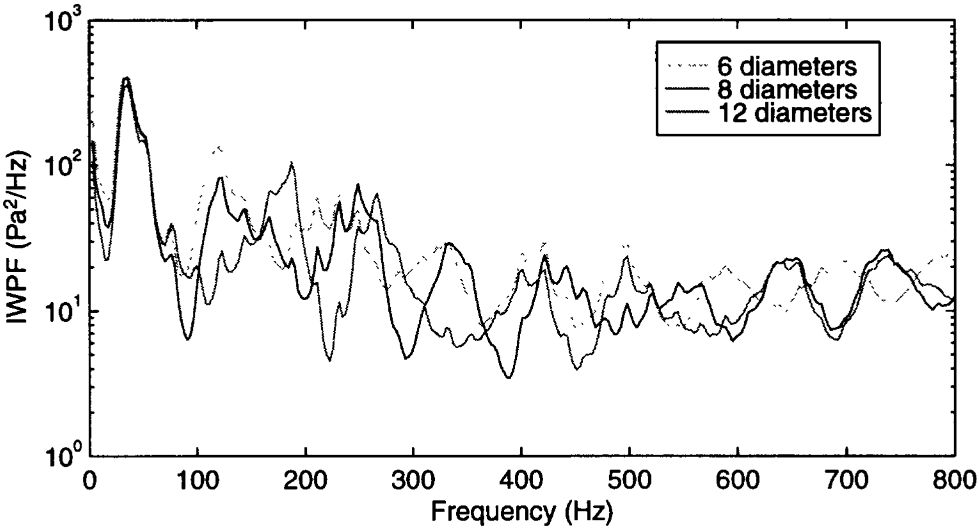

Figure 7 Autospectra at 6, 8 and 12 diameters for 0 to 800 Hz with anechoic termination end condition

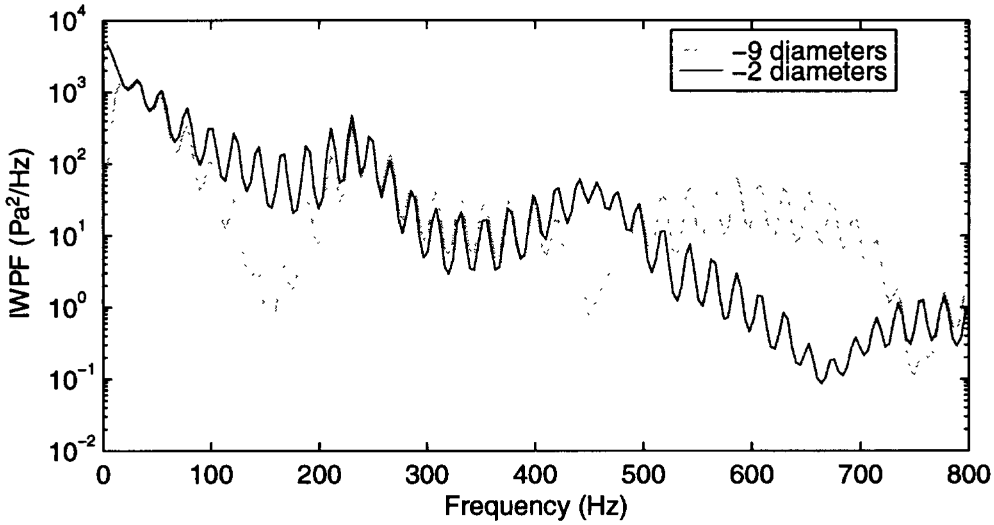

Figure 8 Typical autospectra at -9 and -2 diameters for 0 to 800 Hz

Typical autospectra at -9 and -2 diameters are given in Figure 8 and these are indeed similar in character to those evident in Figure 7. As there is no mismatching of the peaks in Figure 8, it is suggested that the cause of this narrow peak - trough character is due to a flow disturbance upstream of -9 diameters which creates this phenomenon and then projects sound down the pipe. Had the narrow band peaks been localised there would have been some alteration in their character.

The coherence for 180° angular separations have been measured at each of the two upstream measurements locations and for most frequencies the coherence is almost unity. This high coherence is only reduced at frequencies with very low signal energy where background noise becomes significant. In addition an examination of the coherence between -9 and -2 diameters also revealed near unity coherence for frequencies at which both signals were of reasonable magnitude. This suggests that it is correlated phenomena which dominate the wall pressure field upstream of the flow disturbance and not uncorrelated phenomena such as hydrodynamic turbulence and broadband noise.

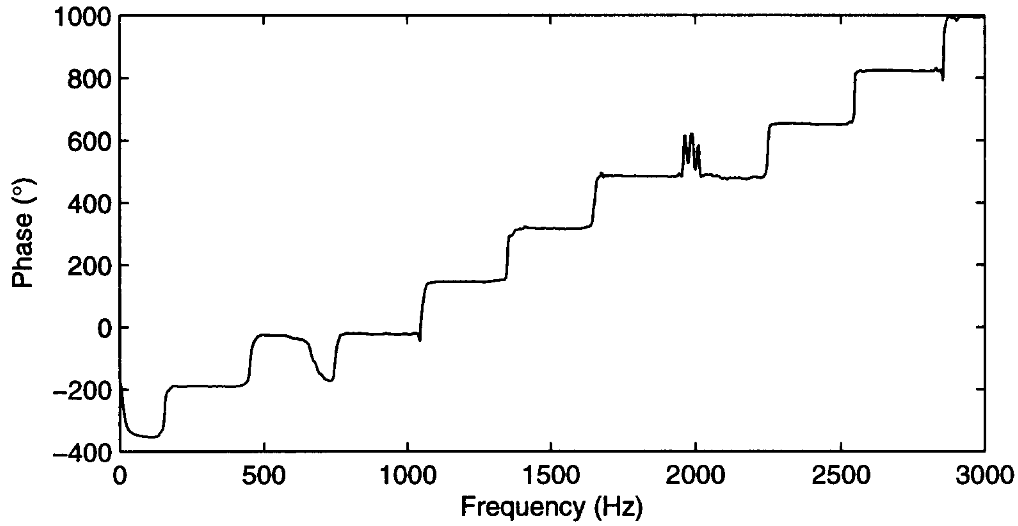

Figure 9 Typical unwrapped phase of the cross spectrum between -9 and -2 diameters

The unwrapped phase may then be used as a diagnostic tool to identify the nature of the signal energy. The unwrapped phase between -9 and -2 diameters is given in Figure 9 and reveals two features. Firstly the unwrapped phase rises at a steady gradient. This gradient is linked to the time delay for the signal energy propagating between the measurement locations. Secondly the unwrapped phase contains numerous rises and falls of 180°.

The 180° rises and falls in Figure 9 occur whenever the transfer function between the two measurement locations passes through either a pole or a zero. It is suggested that these 180° phase shifts occur as the result of the two measurement locations moving in and out of phase with each other as the frequency band is swept. This is the result of a modal pattern occurring within the duct. At a particular frequency the modal content of the signal will therefore either be in or out of phase by 180°. This portion of the signal is stationary (time unaffected) and so is unaffected by the juxtaposed propagating component.

Lyon[6] describes the phase relationship between source and receiver for a one dimensional acoustic pipe and describes the effect this relationship has on the phase component of the transfer function. Lyon[6] states that the average phase delay for some high frequency may be considered by counting the number of poles and zeroes.

From equation 7.17 in Lyon[6]

$$\phi = (N_{poles} - N_{zeroes}) \cdot \pi = k(x_o - x_s) \qquad (2)$$

Clearly this argument may be extended to transfer functions between two receiver locations. For locations x_1 to x_2 and sound propagation speed v, from equation 2.

$$\phi(f) = (N_{poles} - N_{zeroes}) \cdot \pi = \frac{2\pi f}{v}(x_2 - x_1) \qquad (3)$$

In practice from a plot of the unwrapped phase the average phase delay may then be considered as a line between the phase value at a start frequency (0 Hz for example) and the phase value at a finish frequency. The gradient of this line is then the average time delay as per equation 1.

From Figure 9 taking the phase difference between 0 and 3000 Hz. and using equation 1.

$$\tau = \frac{\Delta\theta}{360 \cdot \Delta f} = \frac{1370}{360 \cdot 3000} = 1.27x10^{-3} \ \ \text{sec}$$

$$\Rightarrow v \approx \frac{\Delta x}{\tau} = \frac{7x0.0627}{1.27x10^{-3}} \approx 350 \ \ m/\text{sec}$$

It is clear that the energy is propagating from the upstream to the downstream direction and that this is due to acoustic energy propagating down the pipe from some upstream source towards the orifice. The propagation speed should be the speed of sound plus the flow speed which for 16°C and a Mach number of 0.07 = 1.07 x 341 = 365 m/s. Whilst the calculated and measured results are not in exact agreement the nature of the propagation is evident by elimination of the other possibilities (upstream acoustic propagation or correlated downstream hydrodynamic propagation dominating).

Based on the above analysis there exists within the upstream section of pipe a predominantly acoustic field consisting of a standing wave field and also a propagating wave field which is the sum of many frequencies which have a small peak to peak frequency difference.

TRANSMISSION OF ENERGY THROUGH THE ORIFICE

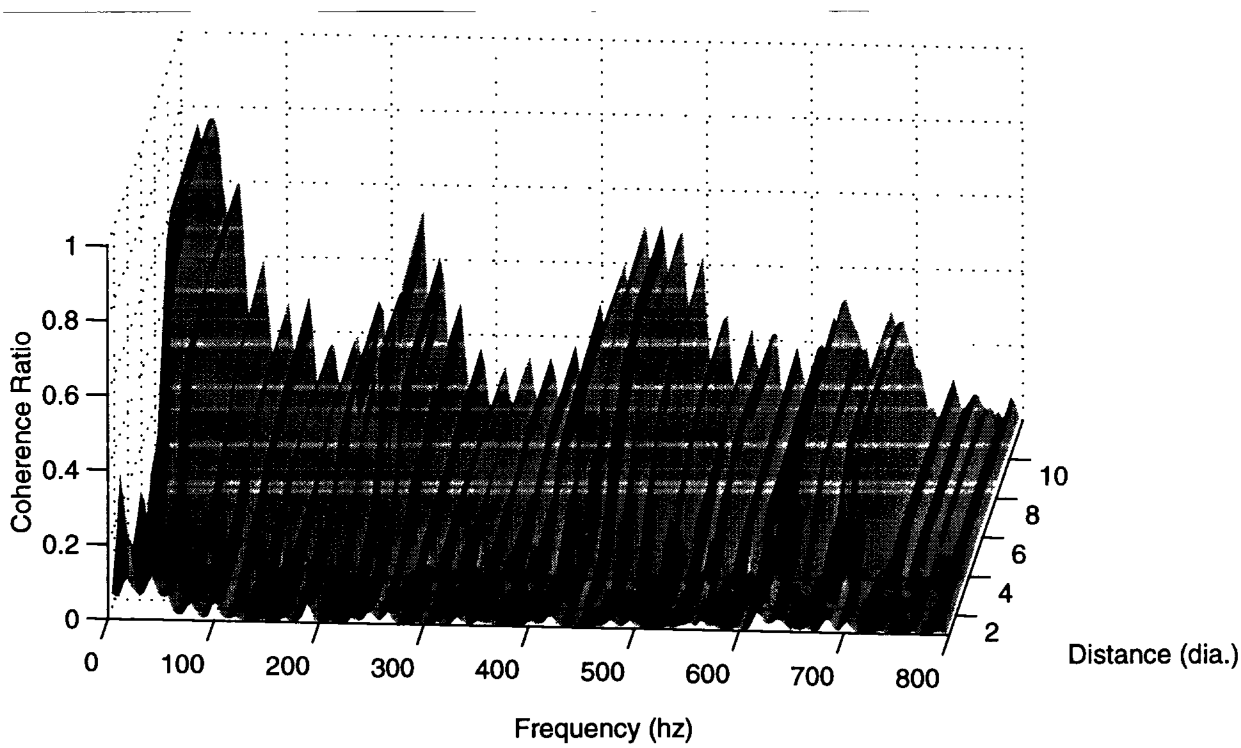

Figure 10 Coherence measured between -2 and 1, 2, 3, 4, 5, 6, 8 and 12 diameters with the anechoic termination end condition

In order to determine whether the similarity between the upstream and downstream acoustic fields was due to the transmission of energy across the orifice, a single input - single output linear relationship was assumed between -2 diameters and each downstream location. The coherences for these relationships are presented in Figure 10.

Firstly it is clearly evident from Figure 10 that there is significant coherence between -2 diameters and the downstream axial locations. Namely that there is a relationship between the upstream and downstream acoustic fields for both flow conditions, and that this relationship may be expressed as a single input - single output linear system.

The second feature of the results in Figure 10 is that the coherences from -2 diameters to the downstream locations are weaker closer in to the orifice plate and then steadily improve with distance away from the orifice. There could be a number of reasons for this: i) There are significant non-correlated fluctuations at the axial distances close to the orifice. This was evident in the coherences obtained across the diameter of the duct as presented in Figure 3. ii) The sound could be being projected away from the axial locations at close proximity to the orifice if the separated flow region is acting as a wave guide of the acoustic energy and iii) The relationship between the acoustic energy close in to the orifice is actually nonlinear and it is only when the flow field has redeveloped that a linear relationship re-establishes itself.

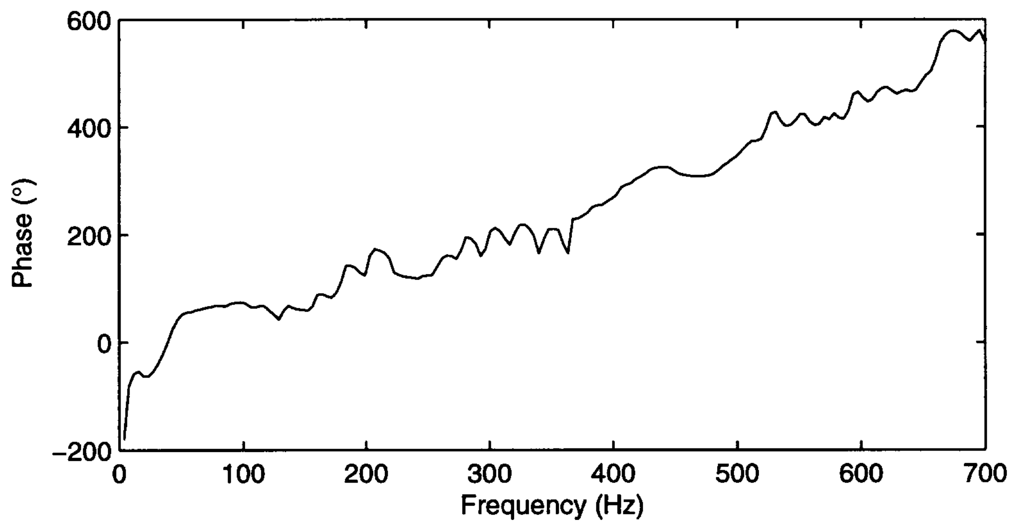

Figure 11 Unwrapped phase of the cross spectrum from -2 diameters to 12 diameters with the anechoic termination end condition

The unwrapped phase between -2 and 12 diameters was determined (Figure 11) to identify the nature of the relationship between the observed spectral peaks. From equation 1 and the speed, distance, time relationship.

$$\tau = \frac{\Delta\theta}{360 \cdot \Delta f} = \frac{650}{360 \cdot 700} = 2.58x10^{-3} \ \text{sec}$$

$$\Rightarrow v \approx \frac{\Delta x}{\tau} = \frac{14x0.0627}{2.58x10^{-3}} \approx 340 \ \ m/\text{sec}$$

As with the propagation speed determined from Figure 9 whilst a faster propagation speed was anticipated, the nature of the relationship is clearly due to a downstream propagating acoustic field. This is determined by the positive gradient of Figure 11 and the magnitude of the result precluding other options.

CONCLUSIONS

An examination has been made of the internal wall pressure fluctuations at various axial locations downstream of an orifice plate for a fixed mass flow rate for one orifice size with an anechoic termination and open flanged end conditions.

The autospectra of these fluctuations for frequencies below the onset of the (1,0) higher order acoustic mode gives the form of the fluctuations with increasing distance downstream of the orifice plate. The conclusion made in Pedersen and Norton[1] that the wall pressure field made a transition from one dominated by uncorrelated turbulent fluctuations to a propagating acoustic field was supported by coherences for 180° angular separations and by using unwrapped phase analysis

Examination was made of the effect of an imposed standing wave field on this system by removing the attached anechoic termination. The standing wave field has a profound effect on the frequency distribution of the internal wall pressure fluctuations particularly downstream of reattachment. This has major implications for acoustic fatigue in industrial piping.

Using the cross spectra method for 180° angular separations, the portion of the autospectra due to turbulent fluctuations may largely be removed to reveal that part of the signal which contains the correlated phenomena. This confirmed the presence of the standing wave field within the separated flow region for the flanged pipe end condition.

After noting a similarity between portions of the autospectra for the upstream and downstream acoustic fields, the existence of a relationship between these two fields was examined using coherence functions and unwrapped phase. This relationship is due to a downstream propagating acoustic field that is transmitted through the orifice.

REFERENCES

1. PEDERSEN, R.C. & NORTON, M.P. 1997, Quantification of acoustic and hydrodynamic fields in flow duct systems, *Applied Acoustics*, **50**(3), 205-230.
2. KERSCHEN, E.J. & JOHNSTON, J.P. 1981 Modal content of noise generated by a coaxial jet in a pipe. *J. Sound & Vibration*, **76**(1), 95-115.
3. AGARWAL, N.K. 1994 The sound field in a fully developed turbulent pipe flow due to internal flow separation, Part I:Wall-pressure fluctuations, *J. Sound & Vibration*, 169(1), 65-76.
4. STAHL, B. 1987 An experimental investigation of noise generated by turbulence in a pipe flow downstream of a discontinuous area enlargement. *European Space Agency Technical Translation*, ESA-TT-996.
5. PEDERSEN, R.C. & NORTON, M.P. 1996 Use of the unwrapped phase spectrum in identifying propagating plane waves in industrial piping systems from measured data, *First Australasian Congress on Applied Mechanics*, Melbourne, Australia, 807-812.
6. LYON, R.H. 1987 Machinery Noise and Diagnostics, Butterworth Publishers.